Studies on the room temperature growth of nanoanatase phase Ti O 2 thin films by pulsed dc magnetron with oxygen as sputter gas

A. Karuppasamy and A. Subrahmanyam

Citation: Journal of Applied Physics **101**, 064318 (2007); doi: 10.1063/1.2714770
View online: http://dx.doi.org/10.1063/1.2714770
View Table of Contents: http://scitation.aip.org/content/aip/journal/jap/101/6?ver=pdfcov
Published by the AIP Publishing

Studies on the room temperature growth of nanoanatase phase TiO_2 thin films by pulsed dc magnetron with oxygen as sputter gas

A. Karuppasamy[a] and A. Subrahmanyam
Semiconductor Laboratory, Department of Physics, Indian Institute of Technology Madras, Chennai 600036, India

(Received 19 November 2006; accepted 24 January 2007; published online 28 March 2007)

The anatase phase titanium dioxide (TiO_2) thin films were deposited at room temperature by pulsed dc magnetron sputtering using pure oxygen as sputter gas. The structural, optical, electrical, and electrochromic properties of the films have been studied as a function of oxygen pressure in the chamber. The x-ray diffraction results indicate that the films grown above 4.5×10^{-2} mbar are nanocrystalline (grain size of 28–43 nm) with anatase phase. The films deposited at the chamber pressure of 7.2×10^{-2} mbar are found to be highly crystalline with a direct optical band gap of 3.40 eV, refractive index of 2.54 (at $\lambda=400$ nm), and work function of 4.77 eV (determined by the Kelvin probe measurements). From the optical emission spectra of the plasma and transport of ions in matter calculations, we find that the crystallization of TiO_2 at room temperature is due to the impingement of electrons and ions on the growing films. Particularly, the negative oxygen ions reflected from the target by "negative ion effects" and the enhanced density of TiO, TiO^+, TiO_2^+, and O^{2+} particles in the plasma are found to improve the crystallization even at a relatively low temperature. From an application point of view, the film grown at 7.2×10^{-2} mbar was studied for its electrochromic properties by protonic intercalation. It showed good electrochromic behavior with an optical modulation of ~45%, coloration efficiency of 14.7 $cm^2\,C^{-1}$, and switching time (t_c) of 50 s for a 2×2 cm^2 device at $\lambda=633$ nm. © *2007 American Institute of Physics*.
[DOI: 10.1063/1.2714770]

I. INTRODUCTION

In recent years, crystalline and nanocrystalline titanium dioxide (TiO_2) thin films have attracted considerable attention due to their potential applications in a wide range of fields such as photocatalysis, electrochromism, solar cells, gas sensors, self-cleaning windows, and dielectric thin film capacitors.[1–6] It is well known that TiO_2 crystallizes in anatase, rutile, and brookite structures, among which, most of the above said applications comes from the anatase phase of TiO_2. In general, the as-deposited TiO_2 films are amorphous in nature and hence the crystallization of TiO_2 is done either by postannealing or by substrate heating.[7] However, the recent applications of TiO_2 such as in flexible electronics, antireflection coating on plastic lenses, etc., demand the films to be coated on heat sensitive substrates at room temperature (300 K). So, growth of anatase phase TiO_2 thin films at low temperatures (~300 K) is a desired requirement. Attempts have been made to realize the crystallization of anatase phase of TiO_2 at low temperatures by various methods such as sol-gel, wet oxidation, etc.[8–10] One of the techniques to achieve the anatase phase is to sputter (either dc or rf) titanium metal or titanium dioxide targets with oxygen as the sputter gas.[11–14] It is known that dc sputtering of metallic titanium with pure oxygen leads to target poisoning and rf sputtering suffers from low deposition rate. We have overcome many of these problems encountered in the conventional dc and rf sputtering by using pulsed dc magnetron sputtering. The advantages of the pulsed dc magnetron sputtering with oxygen as sputter gas has been demonstrated in our recent work.[15] It may be mentioned here that the TiO_2 thin films grown by pulsed dc magnetron sputtering are found to be anatase and nanocrystalline in structure and have better electrochromic properties. Thus, the aim of the present investigation is (i) to synthesize nanoanatase phase TiO_2 thin films at room temperature (300 K) by pulsed dc magnetron sputtering of titanium metal in pure oxygen plasma and (ii) to study the effect of oxygen sputter pressure on the composition and physical properties (structural, optical, electrical and morphological) of TiO_2 thin films. Additionally, the oxygen plasma has been analyzed using transport of ions in matter (TRIM) calculations and optical emission spectroscopy (OES) and in an application point of view, the electrochromic property of the films has also been investigated.

II. EXPERIMENTAL DETAILS

A. Preparation of thin films

The titanium dioxide thin films are grown on indium tin oxide (ITO) coated glass, quartz, and single crystal silicon substrates (100) by reactive pulsed dc magnetron sputtering of metallic titanium using pure oxygen as sputter gas. The circular magnetron cathode (7.4 cm diameter) is designed and fabricated "in house." The sputter chamber is initially evacuated to a base pressure of 2.0×10^{-6} mbar and then pure oxygen gas is introduced into the chamber through mass flow controller (UNIT, Model UFC 180) and the chamber pressure is measured using a combination vacuum gauge

[a]Author to whom correspondence should be addressed; FAX: +91-44-22574852; electronic mail: ksamy@physics.iitm.ac.in

(Leybold, Ionivac ITR90). Three sets of samples, namely, S1, S2, and S3 have been prepared at three chamber pressures (with different flow rates of oxygen) of 0.9×10^{-2}, 4.5×10^{-2}, and 7.2×10^{-2} mbar, respectively. After the oxygen flow is stabilized in the chamber, the target is powered through a pulsed dc magnetron power supply (Advanced Energy, Model MDX 500 and MDX sparc-LE 20) operating in constant power mode at 7.0 W/cm^2 (the voltage and the current of the target have been recorded during the sputtering process). The deposition time for all the films was kept constant at 1.0 h. Before every sputtering run, the targets have been presputtered with argon gas for 5 min in order to ascertain the same state of the target in every run.

B. Plasma diagnosis

During the sputtering process, the optical emission spectrum of the oxygen plasma was recorded using a fiber optic spectrophotometer (Ocean Optics-HR2000) interfaced to a computer; data are analyzed using Ocean Optics SPECLINE database package.

C. Characterization of TiO_2 thin films

The crystalline nature of TiO_2 thin films were investigated by an x-ray diffractometer (Shimadzu, XD-D1) using Cu $K\alpha$ radiation, and the grain size was calculated using Scherrer's formula. The surface morphology of the films has been evaluated by on atomic force microscope (Digital Instruments Nanoscope IV). The optical transmittance measurements on the grown TiO_2 thin films were carried out with a double beam spectrophotometer (Jasco V-570) in the wavelength range of 350–850 nm. The thickness (to an accuracy of ±5 nm) and refractive index (±5%) of the films have been evaluated from the reflectance spectra using Filmetrics-F20. The four probe electrical resistivity measurements have been carried out using an electrometer (Keithley-614). The surface work function/contact potential difference (V_{CPD}) between the TiO_2 films and the stainless steel reference electrode (Φ_R=4.81 eV) has been measured by an indigenously designed and fabricated reed-type Kelvin probe;[16] the accuracy of the measurement is within 0.001 eV. The electrochemical coloration/decoloration was done using a programmable electrochemical workstation (CH instruments, CHI660B).

III. RESULTS AND DISCUSSION

A. Structure and morphology

The x-ray diffractograms of the TiO_2 thin films deposited at various chamber pressures are shown in Fig. 1. As may be seen, the films formed at low chamber pressure of 0.9×10^{-2} mbar are amorphous; while the films grown at higher chamber pressures of 4.5×10^{-2} mbar and above are crystalline and have anatase phase.[28] With an increase in the sputter gas pressure, the preferential Bragg peak intensity of (101) plane is found to be more than that of the (200) plane; this observation is in agreement with the earlier report[14] and is attributed to the difference in surface formation energy of various TiO_2 phases and their planes. The surface formation

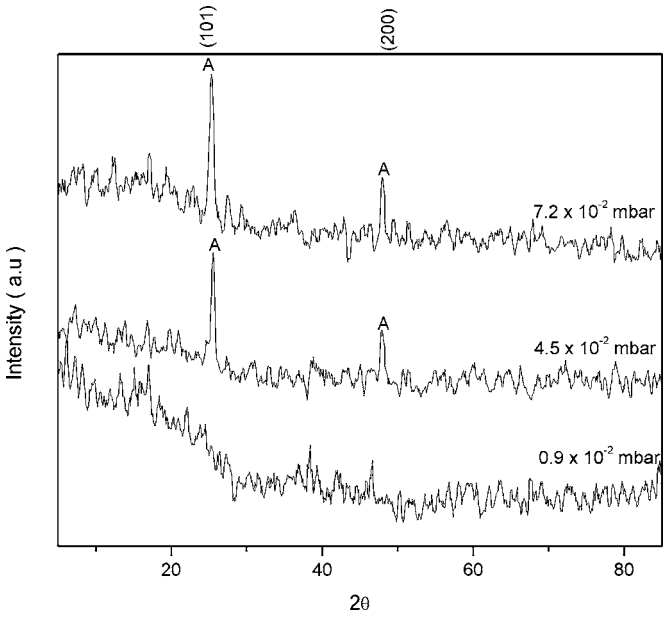

FIG. 1. The x-ray diffractograms of the TiO_2 films deposited on quartz substrates under different oxygen sputter pressures.

energy of anatase phase is 0.44 J/m^2 for (101) plane and 0.53 J/m^2 for (200) plane.[17] From the full width at half maximum, the average crystallite sizes determined by Scherrer's formula for S2 and S3 are found to be 28.3 and 35.6 nm, respectively. These values are in fair agreement with the surface crystallite size measured by atomic force microscopy (AFM). Figure 2 shows the surface morphology of samples S2 and S3 studied by atomic force microscopy. The surface of the films S2 and S3 are smooth, dense, and compact with a root mean square surface roughness of 5 and 9 nm and average surface crystallite size of 24 and 43 nm, respectively. The crystallization of TiO_2, though, is confirmed by x-ray diffraction (XRD) and AFM; the source of crystallization energy for the agglomeration of TiO_2 thin films requires more attention and detailed explanation. The two possible processes that crystallize the film during sputter deposition are (i) the thermal energy induced by substrate heating and (ii) the energy of sputtered particles (electrons, ions, and neutral species) impinging on the film surface. In the present experiment, the substrate is not intentionally heated and the rise in substrate temperature due to the sput-

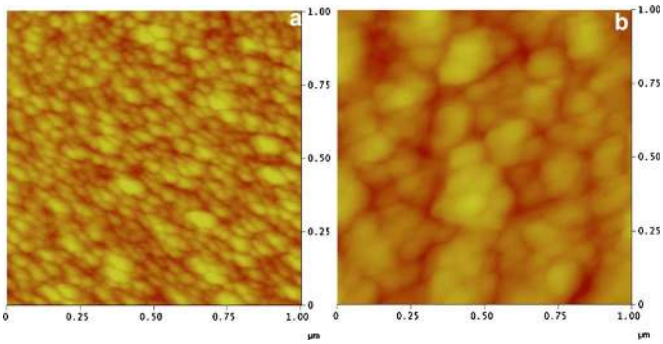

FIG. 2. (Color online) Two-dimentional (2D) representations of atomic force microscopy (AFM) pictures recorded for the TiO_2 thin films prepared at (a) 4.5×10^{-2} mbar and (b) 7.2×10^{-2} mbar oxygen pressure.

tering process (energy impact of the secondary electrons) monitored by chromel-alumel thermocouple reached a maximum temperature of 85 °C for a sputtering pressure of 7.2×10^{-2} mbar. Thus, it may be inferred that the crystalline formation of TiO_2 by oxygen sputtering is not due to the thermal process. Therefore, the only other source of energy for crystallization is the sputtered particles impinging on the film surface; the details are discussed below.

The sputtering power is kept constant throughout the experiments. With an increase in the sputtering pressure from 0.9×10^{-2} to 7.2×10^{-2} mbar, a fall in sputtering voltage from 540 to 470 V is observed. This means that the particles sputtered at low pressure have higher energy. At high pressures the sputtered species have low energies due to large number of collisions. Therefore, the crystallization at high sputtering pressure cannot be related to the energy of the sputtered particles, particularly the neutral radicals. However, the electrons and negative ions formed very near the target surface are accelerated across the sheath potential and reach the film surface to impart energy to the growing films. At larger sputtering pressures, these species have comparatively less energy but their density is very high, and so they are found to be the probable species for crystallization. The most likely species that can be formed near the target during oxide deposition are the negative oxygen ions; these ions are accelerated across the sheath and subsequently neutralized in the plasma. They have a high kinetic energy and a small scattering cross section and, therefore, will reach the substrate and impart energy to the film growing on it. This phenomenon is reasonably well known as "negative ion effect" in the sputter deposition of highly oxygenated targets.[18] Salinga *et al.*[19] have reported similar observation of oxygen ion imparting energy to the growing film of WO_3. There are other reports saying that the energy of the particles impinging on the substrate determines the formation of amorphous or crystalline TiO_2.[12] This is a general conclusion to which we would like to add that the dominant species imparting energy to the growing film during oxygen sputtering are the negative oxygen ions formed very near the target surface. To verify this, we have performed TRIM calculations for high energetic oxygen ion bombardment on TiO_2 film and on metallic titanium target.

1. TRIM calculations

In the present study, the crystallization of titanium dioxide is presumed to be caused by oxygen ion bombardment on the growing films. Particularly, the energy and density of the oxygen ions bombarding the growing film are expected to induce crystallization. So, in order to determine (i) the relative number of oxygen ions reflected from the target and (ii) the effect of oxygen ion bombardment on the growing film, TRIM calculations for 10 000 oxygen ions bombarding semi-infinite titanium and TiO_2 targets with energies 0.54–0.47 K eV (corresponding to different chamber pressures) have been performed.

(i) The relative number of oxygen ions reflected from the target. Generally, in TRIM calculations the path of an ion within a target material is tracked. As it is known, the collisions with the target atoms cause energy and momentum

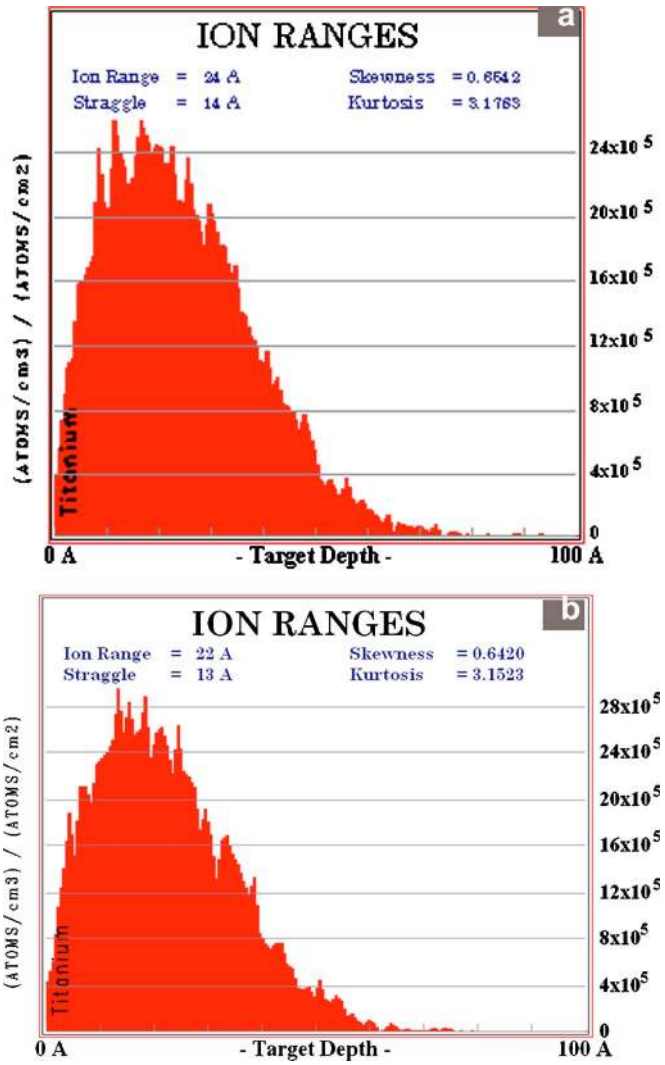

FIG. 3. (Color online) Oxygen ion distributions in titanium metal target calculated using SRIM 2003 at a sputter pressure of (a) 0.9×10^{-2} mbar and (b) 7.2×10^{-2} mbar.

transfer which leads to the reduction of energy of the incident ion and a change of its direction. For sufficient momentum transfer, the target atom itself may move within the solid and cause further collisions. These cascades are tracked until all particles involved are resting.[19] The above calculations have been performed using the TRIM program SRIM 2003. The distributions for oxygen ion ranges in the titanium metal are shown in Figs. 3(a) and 3(b). The calculation results in the following values for the number of oxygen ions reflected at sputter pressures of 0.9×10^{-2} and 7.2×10^{-2} mbar. For S1, the number of backscattered oxygen ions is 1334 and the O-ion range is 24±14 Å. For S3, the number of backscattered oxygen ions is 1443 and the O-ion range is 22±13 Å. These values indicate that more number of oxygen ions is reflected from the target at higher sputtering pressure, and we also find that the range of oxygen ion is very less and hence have a higher probability of getting released from the target. Overall, the density of oxygen ions reflected from the surface is found to be larger at higher oxygen pressures.

(ii) Effect of oxygen ion bombardment on the growing film. Figures 4(a)–4(d) show the distribution of oxygen ion

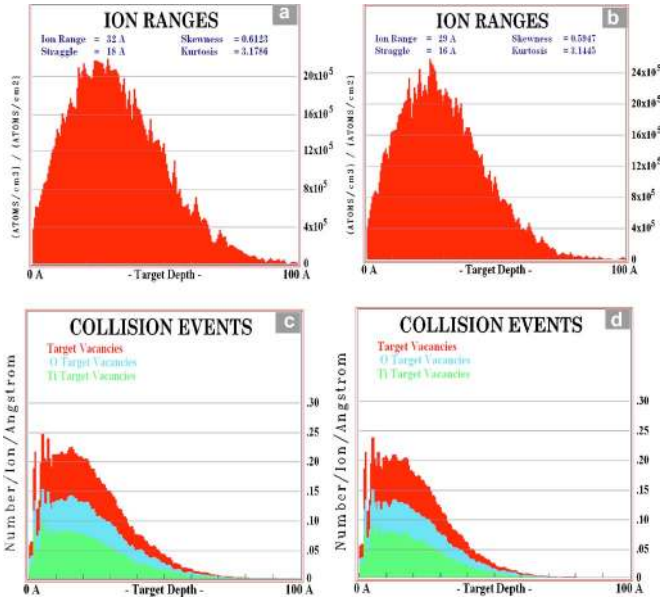

FIG. 4. (Color online) TRIM calculations on oxygen ion distributions [(a) and (b)] and vacancies [(c) and (d)] in titanium dioxide thin films carried out using SRIM 2003 at a sputter pressure of 0.9×10^{-2} and 7.2×10^{-2} mbar, respectively.

ranges and vacancies in the TiO_2 film due to oxygen ion bombardment in samples S1 and S3. The calculation results in the following values. For S1, the vacancies per O ion is 8.5 and the O-ion range is 32±18 Å. For S3, the vacancies per O ion is 7.5 and the O-ion range is 29±16 Å. These values indicate that at low sputtering pressure, the oxygen ions have higher energy and penetrate the film to sputter the atoms from the film which leads to more number of vacancies in the film. Whereas, at higher sputtering pressure, the oxygen ions have comparatively less energy and so they transfer their energy to the growing films creating less vacancies and traveling less distance into the film.

From these TRIM calculations, we have shown that the energy and density of oxygen ions bombarding the growing film influences the low temperature crystallization of TiO_2 thin films. The density of oxygen ions reflected from the target shows pressure dependence; i.e., at higher sputter pressures, more oxygen ions get reflected from the target. Thus it may be inferred that higher sputtering pressure is more useful for crystallization. At low sputtering pressure, the TiO_2 thin films exhibited amorphous nature in spite of the fact that the energy of the impinging oxygen ions is higher. The important point to be noted here is that the total number of oxygen ions impinging on the TiO_2 thin films at low pressures is lower by ~0.01% (as shown by the TRIM calculations). Thus the total energy imparted to the growing TiO_2 thin films is effectively less compared to that of higher oxygen pressure. All these results indicate that the low temperature crystallization of TiO_2 at high sputtering pressure (7.2×10^{-2} mbar) is due to the large number of oxygen ions released from target which have energy sufficient to initiate crystallization.

2. OES characterization

To further confirm the pressure dependence of oxygen sputter plasma, we recorded the plasma emission lines using a fiber optic spectrophotometer. Figure 5 shows the optical emission spectra of the sputter plasma as a function of sputtering pressure in the wavelength range of 350–850 nm. The optical emission lines were analyzed using SPECLINE (Ocean Optics) database package and each line is indexed in the sequence; element, ionic state followed by the numerals corresponding to the upper and lower quantum numbers of the transition states. From OES spectra, we find that the emission in the sputter plasma is primarily due to O^{2+} species with intense lines at 529.5 and 563.1 nm. A strong emission corresponding to the neutral oxygen is also observed at 777.19 nm. With increase in sputtering pressure we could observe an increase in the intensity of these lines, which is expected. But interestingly, at higher sputtering pressures, we could observe an additional line corresponding to the TiO emission at 615.9 nm. Similar observation has been reported by Vancoppenolle *et al.*[20] According to them, the density of TiO^+ and TiO_2^+ species in the plasma increases with increase in oxygen sputter pressure. The above results indicate that the low temperature crystallization of TiO_2 thin films at higher sputter pressure could also be due to the enhanced density of plasma species such as TiO, TiO^+, TiO_2^+, and O^{2+}.

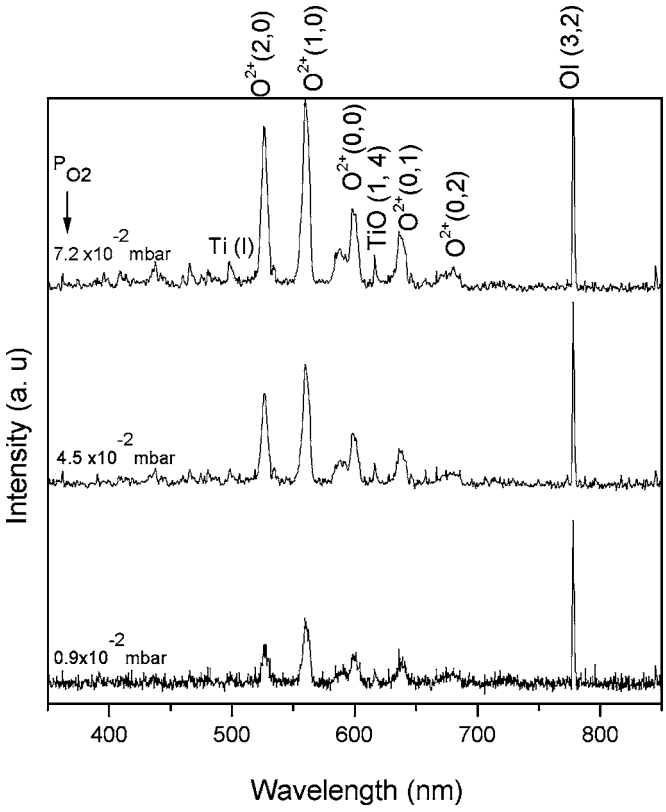

FIG. 5. The optical emission spectra of the oxygen plasma at various oxygen pressures employed for the sputter deposition of TiO_2 thin films.

B. Optical properties

To investigate the effect of oxygen sputtering on the optical properties of TiO_2 thin films, the spectral transmittance and reflectance measurements were performed and the optical parameters such as thickness, band gap, and refractive index were determined. Figure 6 shows the transmittance spectra of the titanium dioxide films deposited onto quartz

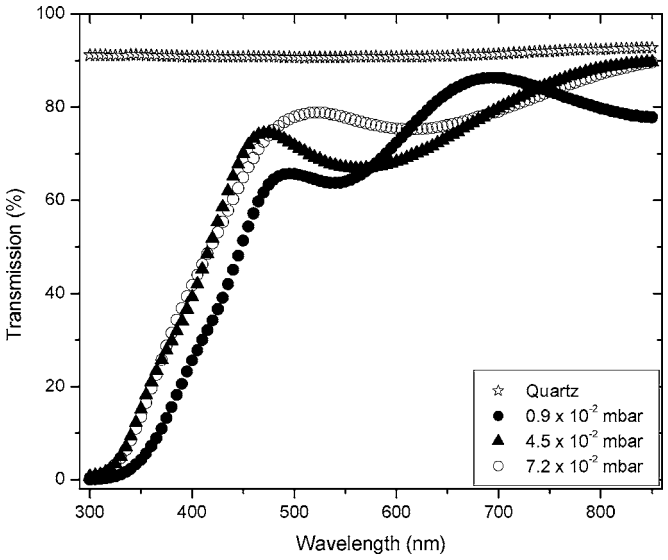

FIG. 6. The optical transmission of TiO_2 thin films deposited at different oxygen pressures in the wavelength range of 300–850 nm.

substrates at different oxygen sputter pressures. The transmittance of the quartz substrate is also given for reference. From the figure, it may be seen that the films deposited at 7.2×10^{-2} mbar exhibit high transparencies (~80%) in the visible and near IR spectral regions whereas the films formed at lower pressures, i.e., 0.9×10^{-2} mbar show lower transmittance (~60% at $\lambda=550$ nm). From the spectra, it may also be observed that the absorption edge is shifted to lower wavelength regions with increase in sputter pressure from 0.9×10^{-2} to 7.2×10^{-2} mbar. Similar results are observed by Asanuma *et al.*[14] To determine the type of band transitions in these oxygen sputtered films, the absorption data were fitted to Tauc's plots and found that there are direct band transitions. The optical band gap of the films is determined by applying the Tauc model[21] in the high absorbance region,

$$\alpha h\nu = A(h\nu - E_g)^n, \tag{1}$$

where $h\nu$ is the photon energy, E_g is the optical band gap, A is a constant and $n=1/2$ for direct transition. Figure 7 shows the $(\alpha h\nu)^2$ versus photon energy plot for these films. The E_g values are estimated as 3.32, 3.38, and 3.43 eV for S1, S2, and S3, respectively. These results are in fair agreement with the band gap values reported by Madhusudan Reddy *et al.* for nanocrystalline TiO_2 thin films.[22] From the reflectance measurements, the thicknesses of the films were estimated to be 313.3, 236.0, and 192.3 nm for S1, S2, and S3 samples, respectively. The variation of refractive index of the films in the spectral range of 400–850 nm as a function of oxygen pressure is shown in Fig. 8. The refractive index of the films agrees with the values reported in the literature.[23] The larger value of n for S3 may be attributed to the improved oxidation and packing density of the sample. But the films prepared at 0.9×10^{-2} show the lowest n values defining the refractive index of porous TiO_2, as determined by the vacancy calculations.

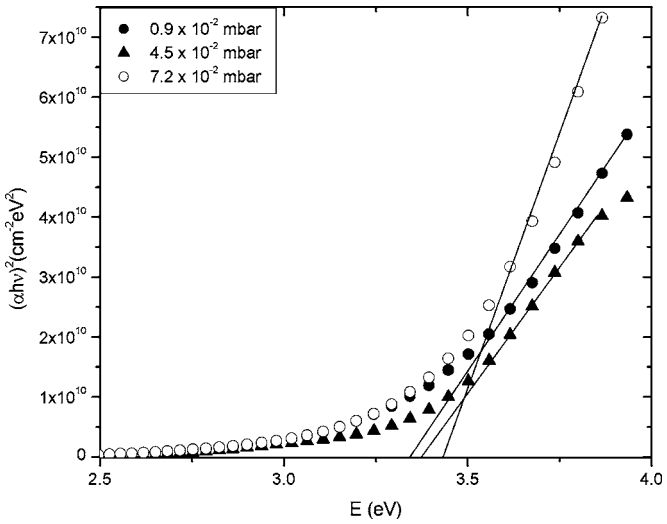

FIG. 7. Tauc's plot of $(\alpha h\nu)^2$ vs incident photon energy for the determination of direct band gap.

C. Electrical properties

In order to determine the activation energy and work function of the oxygen sputtered TiO_2 thin films, the temperature varying resistivity and contact potential difference measurements were performed. Figure 9 shows the temperature dependence of electrical resistivity of TiO_2 films in the temperature range from 300 to 500 K. It may be seen that the TiO_2 films show negative temperature coefficient of resistance (TCR), as anticipated for semiconductors. With rise in sputtering pressure, the electrical resistivity of the films decreases by one order of magnitude, possibly due to the crystallinity improvement.

The activation energies for the oxygen sputtered TiO_2 thin films were calculated using the equation[24]

$$\rho = \rho_0 \exp(E_a/KT), \tag{2}$$

where ρ is the resistivity at temperature T, ρ_0 is a constant, K is the Boltzmann constant, T is the absolute temperature, and

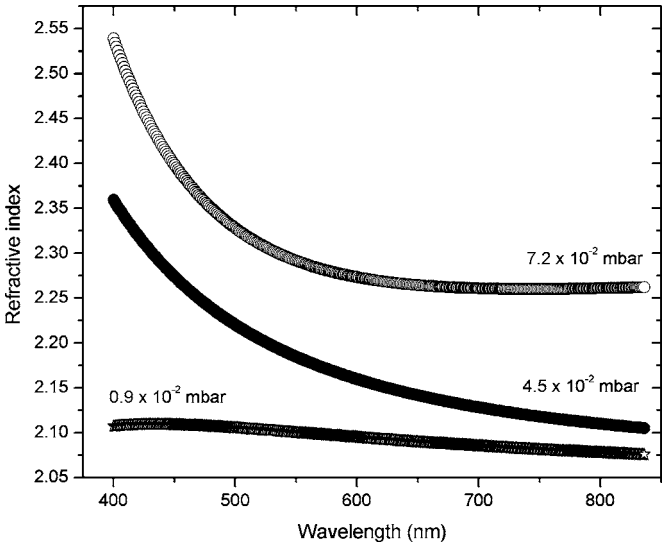

FIG. 8. Variation of refractive index of TiO_2 films as a function of oxygen pressure in the spectral range of 400–850 nm.

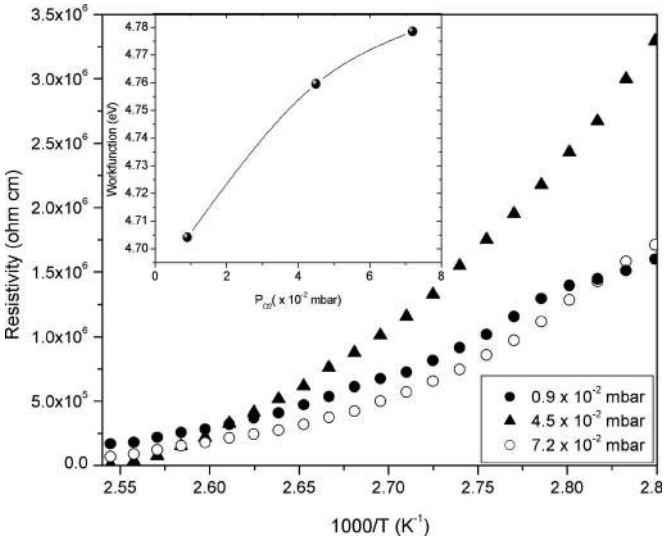

FIG. 9. Temperature dependence of electrical resistivity in the range from 300 to 500 K for the films deposited at various oxygen pressures. (Inset) The work function measured between the TiO_2 thin films and a stainless steel reference electrode as a function of oxygen pressure.

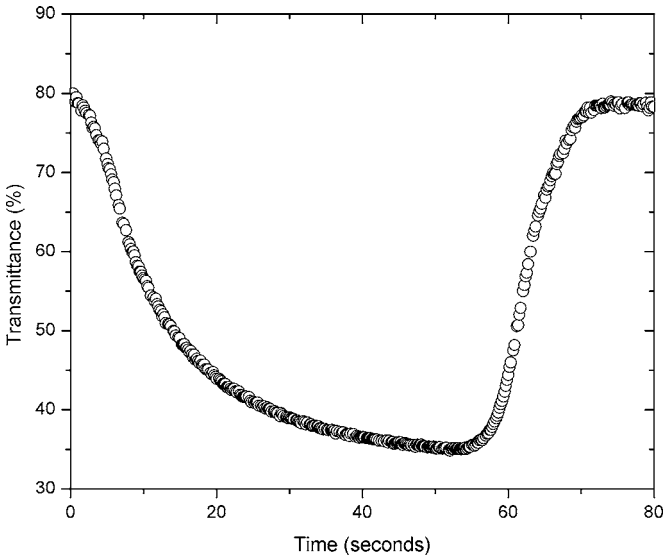

FIG. 10. Variation of transmittance as a function of time in the proton intercalated/deintercalated state of sample S3 at $\lambda = 633$ nm.

E_a is the activation energy. The activation energy thus calculated for the films S1, S2, and S3 are found to be 0.65, 0.80, and 0.86 eV, respectively. These values represent the shallow donor position of the oxygen defect sites below the conduction band and are comparable with the reported values for highly oxygenated titanium dioxide nanoparticles.[25]

The work function of the oxygen sputtered TiO_2 thin films was determined from the contact potential difference (CPD) measurements using Kelvin probe equipment designed and fabricated in house. The Kelvin method of measuring CPD has the advantage that it can be used for a wide range of materials, temperatures, and ambient. The unique feature of this technique is that the surface remains virgin even after the measurement. The basic concept, the design, the fabrication details, and the measurement procedure are given in Ref. 16. All the CPD measurements in the present study are carried out in ambient. The CPD/work function measured for the TiO_2 thin films are reported with the stainless steel reference electrode (work function 4.81 eV). The work function of the film (Φ_F) is calculated using the equation

$$qV_{\mathrm{CPD}} = \Phi_R - \Phi_F, \tag{3}$$

where the work function (Φ_R) of the reference electrode is calibrated using high pure polycrystalline bulk gold sheet by photoemission yield spectroscopy. Work function values determined by the above method were found to be 4.705, 4.750, and 4.779 eV for S1, S2, and S3, respectively [Fig. 9 (inset)]. The higher work function for S3 sample prepared at higher oxygen pressure results in higher resistivity where the Fermi level shifts towards the valence band edge.

D. Electrochromic properties

In an application point of view, the electrochromic property of the films sputter deposited at 7.2×10^{-2} mbar was investigated. To study the coloration behavior, the TiO_2 films were deposited on ITO coated glass substrates with a sheet resistance of 15 Ω/□. The electrochemical insertion/removal of protons was performed in an airtight electrochemical cell composed of the oxide films as working electrode, platinum wire as counterelectrode, and Ag/AgCl as reference electrode. A 0.5*M* HCl dissolved in triple distilled water was used as the electrolyte. The coloration and bleaching potential were kept constant at −3.0 volts and +2.5 V respectively, using a programmable electrochemical workstation. Figure 10 shows the variation of transmittance as a function of time in the intercalated/deintercalated state of sample S3 at $\lambda = 633$ nm. The optical modulation defined as $\Delta T = T_{\mathrm{bleached}} - T_{\mathrm{colored}}$ is reasonably high at 45% and the coloration efficiency (CE) "η" defined as the change in optical density with charges intercalated per unit electrode area is found to be 14.7 $\mathrm{cm^2\,C^{-1}}$ at $\lambda = 633$ nm. The optical modulation and CE are comparable with the reported values of $\Delta T = 37\%$ at $\lambda = 550$ nm (Ref. 3) and CE=9.9 $\mathrm{cm^2\,C^{-1}}$ at $\lambda = 630$ nm.[26] The above results show higher optical modulation and coloration efficiency in oxygen sputtered TiO_2 thin films compared to those prepared by conventional argon sputtering.[27] The real importance of the present work is in the growth of crystalline electrochromic TiO_2 thin films at room temperature.

IV. CONCLUSION

The anatase phase titanium oxide thin films have been prepared at 300 K by pulsed dc magnetron sputtering technique using pure oxygen as a sputter gas. The thickness (313.3–192.3 nm), optical band gap (3.32–3.43 eV), and the work function (4.705–4.779 eV) are found to vary with oxygen pressure in the range of $(0.9–7.2) \times 10^{-2}$ mbar. The films grown above 4.5×10^{-2} mbar chamber pressure are nanocrystalline with anatase phase having a grain size of 28–43 nm. The films grown at higher oxygen sputter pressure (7×10^{-2} mbar) exhibits better electronic properties and good electrochromic performance. The optical modulation

and the coloration efficiency of these films at $\lambda = 633$ nm were found to be 45% and 14.7 $cm^2\ C^{-1}$, respectively. The present investigation clearly shows that the crystallization of nanoanatase TiO_2 films at low temperature is influenced both by the energy impact of the reflected oxygen ions on the growing films and by the enhanced density of plasma species such as TiO, TiO^+ TiO_2^+, and O^{2+}.

[1]S. U. M. Khan, M. Al-Shahry, and W. B. Ingler, Jr., Science **297**, 2243 (2002).
[2]A. Fujishima, K. Hashimoto, and T. Watanabe, TiO_2 *Photocatalysis Fundamentals and Applications* (BKC, Inc., Tokyo, 1999).
[3]A. Verma, S. B. Samanta, A. K. Bakhshi, and S. A. Agnihotry, Sol. Energy Mater. Sol. Cells **88**, 47 (2005).
[4]B. O'Regan and M. Grätzel, Nature (London) **353**, 737 (1991).
[5]W.-P. Tai, J.-G. Kim, and J.-H. Oh, Sens. Actuators B **96**, 477 (2003).
[6]H. K. Ha, M. Yosimoto, H. Koinuma, B.-K. Moon, and H. Ishiwara, Appl. Phys. Lett. **68**, 2965 (1996).
[7]A. Verma, A. Basu, A. K. Bakhshi, and S. A. Agnihotry, Solid State Ionics **176**, 2285 (2005).
[8]J. Musil, D. Heřman, and J. Šícha, J. Vac. Sci. Technol. A **24**, 521 (2006).
[9]Y. Hu and C. Yuan, J. Cryst. Growth **274**, 563 (2005).
[10]K.-S. Lee and I.-S. Park, Scr. Mater. **48**, 659 (2003).
[11]S. Takeda, S. Suzuki, H. Odaka, and H. Hosono, Thin Solid Films **392**, 338 (2001).
[12]P. Löbl, M. Huppertz, and D. Mergel, Thin Solid Films **251**, 72 (1994).
[13]M. D. Wiggins, M. C. Nelson, and C. R. Aita, J. Vac. Sci. Technol. A **14**, 772 (1996).
[14]T. Asanuma, T. Matsutani, C. Liu, T. Mihara, and M. Kiuchi, J. Appl. Phys. **95**, 6011 (2004).
[15]A. Subrahmanyam, A. Karuppasamy, and C. Suresh Kumar, Electrochem. Solid-State Lett. **9**, H111 (2006).
[16]C. Suresh Kumar, A. Subrahmanyam, and J. Majhi, Rev. Sci. Instrum. **67**, 805 (1996).
[17]M. Lazzeri, A. Vittadini, and A. Selloni, Phys. Rev. B **65**, 119901 (2002).
[18]T. J. Vink, E. P. Boonekamp, R. G. F. A. Verbeek, and Y. Tamminga, J. Appl. Phys. **85**, 1540 (1999).
[19]C. Salinga, O. Kappertz, and M. Wuttig, Thin Solid Films **515**, 2760 (2006).
[20]V. Vancoppenolle, P. Y. Jouan, M. Wautelet, J. P. Dauchot, and M. Hecq, Surf. Coat. Technol. **116–119**, 933 (1999).
[21]J. Tauc, *Amorphous and Liquid Semiconductors* (Plenum, London, 1974).
[22]K. Madhusudan Reddy, S. V. Manorama, and A. Ramachandra Reddy, Mater. Chem. Phys. **78**, 239 (2003).
[23]B. Karunagaran, R. T. Rajendra Kumar, C. Viswanathan, D. Mangalaraj, S. K. Narayandass, and G. Mohan Rao, Cryst. Res. Technol. **38**, 773 (2003).
[24]T. P. Gujar, V. R. Shinde, C. D. Lokhande, R. S. Mane, and S.-H. Han, Appl. Surf. Sci. **250**, 161 (2005).
[25]T. Dittrich, J. Weidmann, F. Koch, I. Uhlendorf, and I. Lauermann, Appl. Phys. Lett. **75**, 3980 (1999).
[26]Z. Wang and X. Hu, Thin Solid Films **352**, 62 (1999).
[27]M. P. Cantao, J. I. Cisneros, and R. M. Torresi, Thin Solid Films **259**, 70 (1995).
[28]JCPDS International Center for Diffraction Data Card No. 89–4921 (unpublished).